RSC Advances

ROYAL SOCIETY OF CHEMISTRY

www.rsc.org/advances

Construction and thermal properties of nano-structure polymer bonded explosives with graphene

Congmei Lin, Guansong He, Jiahui Liu, Liping Pan, Shijun Liu *

1,3,5-triamino-2,4,6-trinitrobenzene (TATB)-based polymer bonded explosives (PBXs) modified with graphene were prepared by the water suspension methods. The effects of coating methods and graphene content on the thermal conduction properties were investigated. Reference raw TATB-based PBX samples were also tested and compared with the results obtained from the nanocomposites filled with graphene. The experimental results indicated that the dispersion and concentration of graphene in the nanomaterials could play an important role in the thermal behaviors. Compared with the nanocomposites with out-coating graphene, the corresponding PBXs with inner-coating graphene presented a higher thermal conductivity due to better dispersion of graphene in the composites with the aid of ultrasound vibration. The nonlinear dependence of the thermal conductivity of TATB-based PBXs on graphene content was observed. When the content of inner-coating graphite came to 2 wt%, the thermal conductivity of TATB-based PBX increased by 105.5%, with the values of 1.122 W/m·K. Agari model was adopted to analyze the thermal behaviors of TATB-based PBXs filled with graphene. With the incorporation of graphene, the thermal conduction mechanism of TATB-based PBXs changed from series model to partial parallel model. Additionally, the testing temperatures had a dual effect on the thermal conductivity of TATB-based PBXs. With increasing temperature, the thermal conductivity initially exhibited a sharp drop, and then a little fluctuation was observed in the temperature range of 50-70 °C. Finally, the thermal conductivity of PBXs reduced with temperature again.

1. Introduction

In recent years, the thermal properties of energetic materials have been widely investigated in the academic and industrial fields. The thermal conductivity of liquid octahydro-1,3,5,7-tetranitro-1,3,5,7-tetrazocine (HMX) has been determined from imposed heat flux non-equilibrium molecular dynamics (NEMD) simulations[1]. The NEMD predictions, which comprise the first reported values for thermal conductivity of HMX liquid, are found to be consistent with measured values for crystalline HMX. A novel data processing technique has been developed to obtain thermal diffusivity, conductivity, and reaction heat release for energetic materials from Sandia Instrumented Thermal Ignition (SITI) experiments heated with a linear ramp temperature boundary condition[2]. The pressed PBX 9502 pellet shows a decrease in thermal conductivity with temperature over the range of 50-270 °C and the results are in reasonable agreement with literature values. The physical properties of RX-55-AE-5, which is formulated from heterocyclic explosive, 2,6-diamino-3,5-dinitropyrazine-1-oxide (LLM-105) and 2.5% Viton A have been investigated by Weese et al.[3] The thermal conductivity of RX-55-AE-5 has been found to be 0.475 W/m·K.

Institute of Chemical Materials, China Academy of Engineering Physics, Mianyang, Sichuan 621900, P. R. China.
E-mail: lsj99@sohu.com, Fax: +86-816-2495856; Tel: +86-816-2489302.

Due to the important roles in their behaviors under thermal loading, improving the thermal conductivity of polymer bonded explosives (PBXs) is of great interest. Generally, PBX is a kind of particle highly filled composite material which is comprised of 90-95% weight of explosive crystals and 5-10% weight of a polymeric binder. Despite the polymer content in PBX being very low[4], the polymer binder plays important roles in the thermal conductivity of PBX. A common and convenient method to enhance the thermal conductivity of polymer is the addition of inorganic nanoparticles, such as graphite, single-walled carbon nanotubes (SWCNTs), multi-walled carbon nanotubes (MWCNTs), and graphene[5-8]. Among the inorganic nanoparticles, as a monolayer of sp^2-hybridized carbon atoms arranged in a two-dimensional lattice, graphene has attracted intensive interest for a variety of applications during the past decade[9-11], due to the exceptional thermal, mechanical, and electrical properties[12-15]. It is recognized that with the addition of a low content of graphene, the thermal conductivity of polymer could be significantly improved. It has been revealed that the thermal conductivity of the graphene/1-octadecanol (stearyl alcohol) nanocomposite increases by nearly 2.5-fold (~140% increase) upon ~4% (by weight) graphene addition[16]. Ganguli et al.[17] have investigated the chemically functionalized exfoliated graphite-filled epoxy composites with load levels from 2% to 20% by weight and found that thermal conductivity of the chemically functionalized graphite/epoxy composite increases by 28-fold over the pure epoxy resin at the 20% by-weight load level, increasing from 0.2 to 5.8 W/m K. Due to that stacking of individual two-dimensional multi-graphene platelets (MGPs) is effectively inhibited by introducing one-dimensional multiwalled carbon nanotubes (MWCNTs), a remarkable synergetic effect between the MGPs and MWCNTs in improving the mechanical properties and thermal conductivity of epoxy composites has been demonstrated[18].

As an insensitive high explosive (IHE), 1,3,5-triamino-2,4,6-trinitrobenzene (TATB) is used in increasing quantities in the military fields due to the extraordinary stability under thermal, impact, or shock-initiation conditions[19-22]. TATB is the energetic constituent in several PBX formulations, such as LX-17 (92.5% TATB and 7.5% a copolymer of chlorotrifluoroethylene and vinylidene fluoride kel-F800 by weight) and PBX-9502 (95% TATB and 5% kel-F800 by weight)[23-25].

Although the graphene has been widely applied to improve the thermal conductivity of polymer composites, its application to PBXs is rarely reported. To improve the thermal conductivity of PBXs, an exploration of nanostructure by the incorporation of graphene seems rather attractive. In this work, TATB-based PBXs filled with different concentrations of graphene were designed and fabricated by water suspension methods. The dispersion of graphene in nanocomposites was observed by a scanning electron microscopy (SEM). The thermal conductivity measurements were performed on the nanomaterials at the temperature range of 20-90 °C. Furthermore, Agari model was used to simulate the thermal conductivity of TATB-based PBXs and analyze the thermal conduction mechanism.

2. Experimental Section

2.1 Materials

1,3,5-triamino-2,4,6-trinitrobenzene (TATB) with a purity of 99%, a specific surface area of 0.87 m^2/g, was synthesized through the amination of TCTNB (1,3,5-trichloro-2,4,6-trinitrobenzene) in the solvent toluene by Institute of Chemical Materials, CAEP, China. A copolymer of chlorotrifluoroethylene and vinylidene fluoride was chosen as the polymer binder, purchased from Zhonghao Chenguang Chemical Industry Co., Ltd. China.

Graphene with 1-5 μm in length and 0.9 nm to 1.2 nm in thickness was provided by Beijing DK Nano Technology Co., Ltd. China. The specific surface area of graphene was higher than 500 m^2/g. The morphology of graphene observed using a scanning electron microscope (SEM) is shown in Fig. 1.The other chemicals and reagents used in this study were commercially purchased and used without further purification.

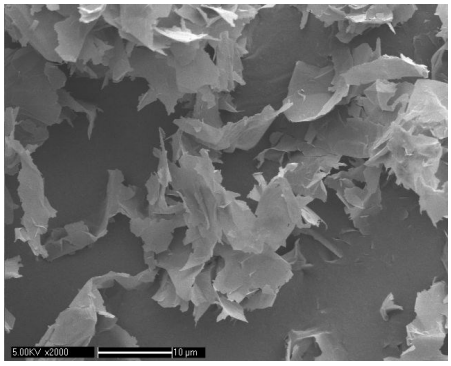

Fig. 1 SEM images of graphene

2.2 Preparation of graphene modified PBXs

The molding powders of TATB-based polymer bonded explosives (PBXs) were prepared with water suspension methods. Graphene modified TATB-based formulations including 5 wt% polymer binder were investigated. The referential formulation, which contained only TATB and fluoropolymer, was labeled as PBX-R. Graphene was coated in the PBXs by two different technologies, i.e. inner-coating and out-coating. During inner-coating technology, graphene was added to a fluoropolymer solution with ethyl acetate and butyl acetate as solvent and dispersed with ultrasound vibration for 15 min. The modified formulations with inner-coating graphene with the addition of 0.05, 0.15, 0.5, 1, and 2 wt% graphene as reinforcing agent were labeled as PBX-I-0.05, PBX-I-0.15, PBX-I-0.5, PBX-I-1, and PBX-I-2, respectively. Then the fluoropolymer solution with graphene was added dropwise to the TATB and H_2O mixture. During out-coating technology, the molding powders of PBX-R was mixed with graphene in a bottom flask and shaken for 15 min. The modified formulations with out-coating graphene with the addition of 0.05, 0.15, 0.5, 1, and 2 wt% graphene as reinforcing agent were labeled as PBX-O-0.05, PBX-O-0.15, PBX-O-0.5, PBX-O-1, and PBX-O-2, respectively. The molding powders were pressed into pellets for thermal conductivity tests.

2.3 Thermal conductivity measurements

The thermal conductivity measurements were conducted with a LFA 447Nanoflash^{TM} laser thermal conductivity apparatus according to GJB-772A-97 standard method 406.2[26]. The specimen dimensions were Φ 12.7 mm × 2 mm. A graphite-coating layer was applied to the pellet materials. The measurements were performed on the nanomaterials at the temperature range of 20-90 °C.

2.4 Morphology observation

Scanning electron microscopy (SEM) measurements were performed with a CamScan Apollo 300 instrument at an operating voltage of 2-10 kV.

3. Results and Discussion

3.1 The effects of coating methods and graphene content

The thermal conductivity of TATB-based PBXs as a function of graphene content at room temperature is demonstrated in Fig. 2. The experimental results show that the thermal conductivity of TATB-based PBXs is improved by the addition of graphene with high thermal conductivity. The results could be attributed to the large contact area between graphene with fluoropolymer matrix which permits ease of heat flows and promoting phonon diffusion in the nanocomposites. Besides, the introduction of inner-coating graphene has a better effect than out-coating graphene to improve the thermal conductivity of TATB-based PBXs. Compared with the TATB-based PBX without graphene, the thermal conductivity of TATB-based PBXs with 2 wt% inner-coating and out-coating graphene increases by 75.6% and 105.5%, with the values of 0.959 W/m·K and 1.122 W/m·K, respectively.

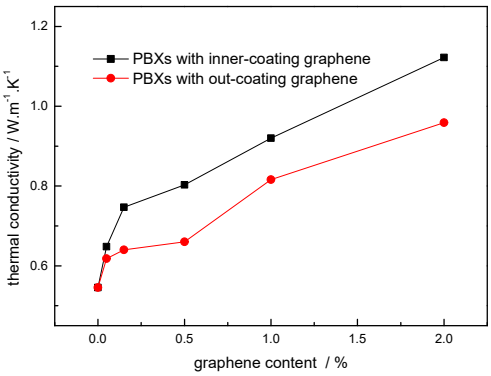

Fig. 2 Plot of thermal conductivity versus graphene content of TATB-based PBXs at 20 °C

The dispersion of graphene are considered here as the key factor for the difference in the thermal conductivity of TATB-based PBXs with inner-coating and out-coating graphene. In order to confirm the dispersion of graphene, a complementary SEM and TEM observation has been applied. Fig. 3 exhibits the SEM and TEM images of graphene/fluoropolymer composites used in the PBXs with inner-coating graphene. The graphene/PF nanocomposites with 1%, 3%, and 10% of graphene (labeled as GP-1, GP-2, and GP-3), corresponding to the concentration in PBX-I-0.05, PBX-I-0.15, and PBX-I-0.5, are prepared by solvent evaporation method after ultrasound vibration for 15 min. It can be found that the graphene particles are fairly well dispersed in the nanocomposites, especially with lower content of graphene (1% and 3%). However, when the graphene filler content further increases to 10%, a small quantity of aggregation could be observed in the nanocomposite, as observed in Fig. 3c and Fig. 3f.

The molding powder and its local enlargement drawings of TATB-based PBXs without and with different content of out-coating graphene are given in Fig. 4. The molding powder out-coated with graphene shows the typical feature of core-shell structure (Figure 4b-f). With 0.05% out-coating graphene, the surface of molding powder was particle coated with graphene. The coverage and thickness of the out-coating graphene shell tend to increase with the content of graphene. The status of graphene coating on the molding powder surface could be observed clearly from the SEM images with high magnification (Figure 4g-l). It can be clearly seen that the graphene form

agglomerates on the surface of molding powder due to the π–π interaction between individual sheet[18]. Therefore, on account of nanosheet aggregation, the thermal conductivity of TATB-based PBXs reduces significantly as compared with the corresponding PBXs with the same content of inner-coating graphene.

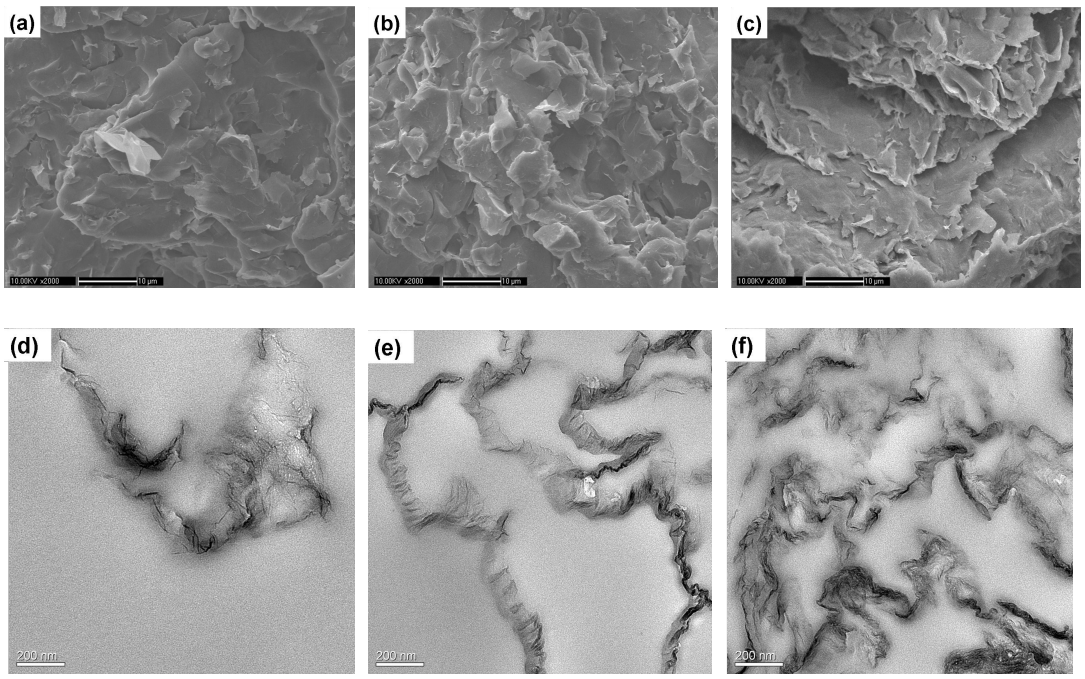

Fig. 3 SEM and TEM images of graphene/fluoropolymer composites: (a) SEM for GP-1; (b) SEM for GP-2; (c) SEM for GP-3; (d) TEM for GP-1; (e) TEM for GP-2; (f) TEM for GP-3.

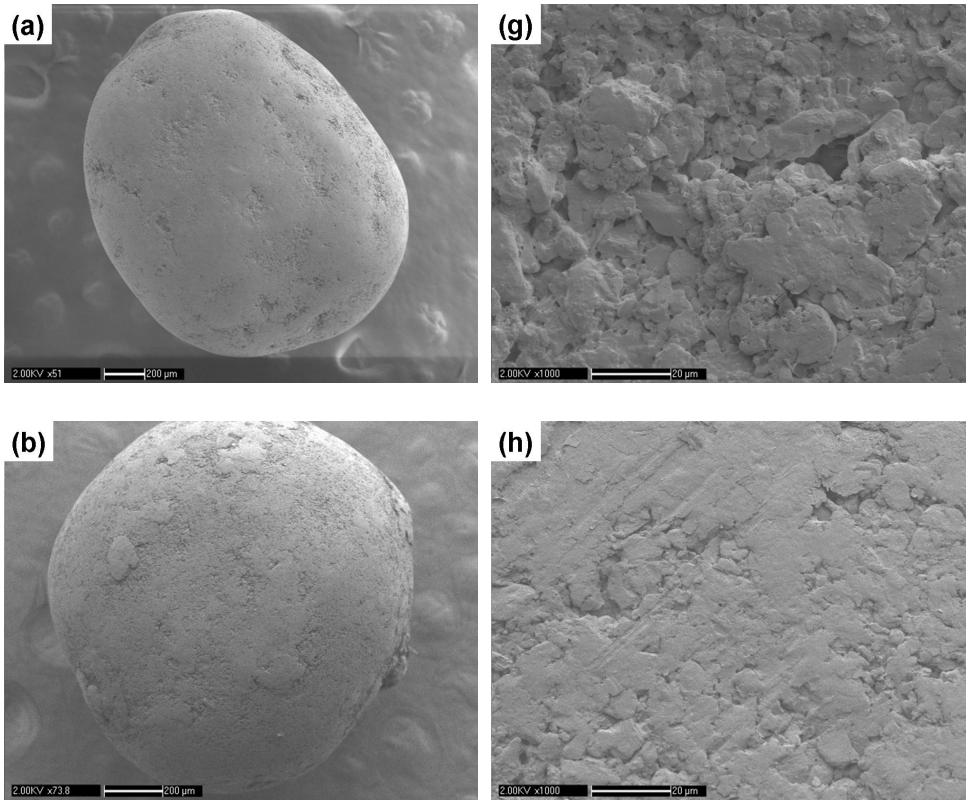

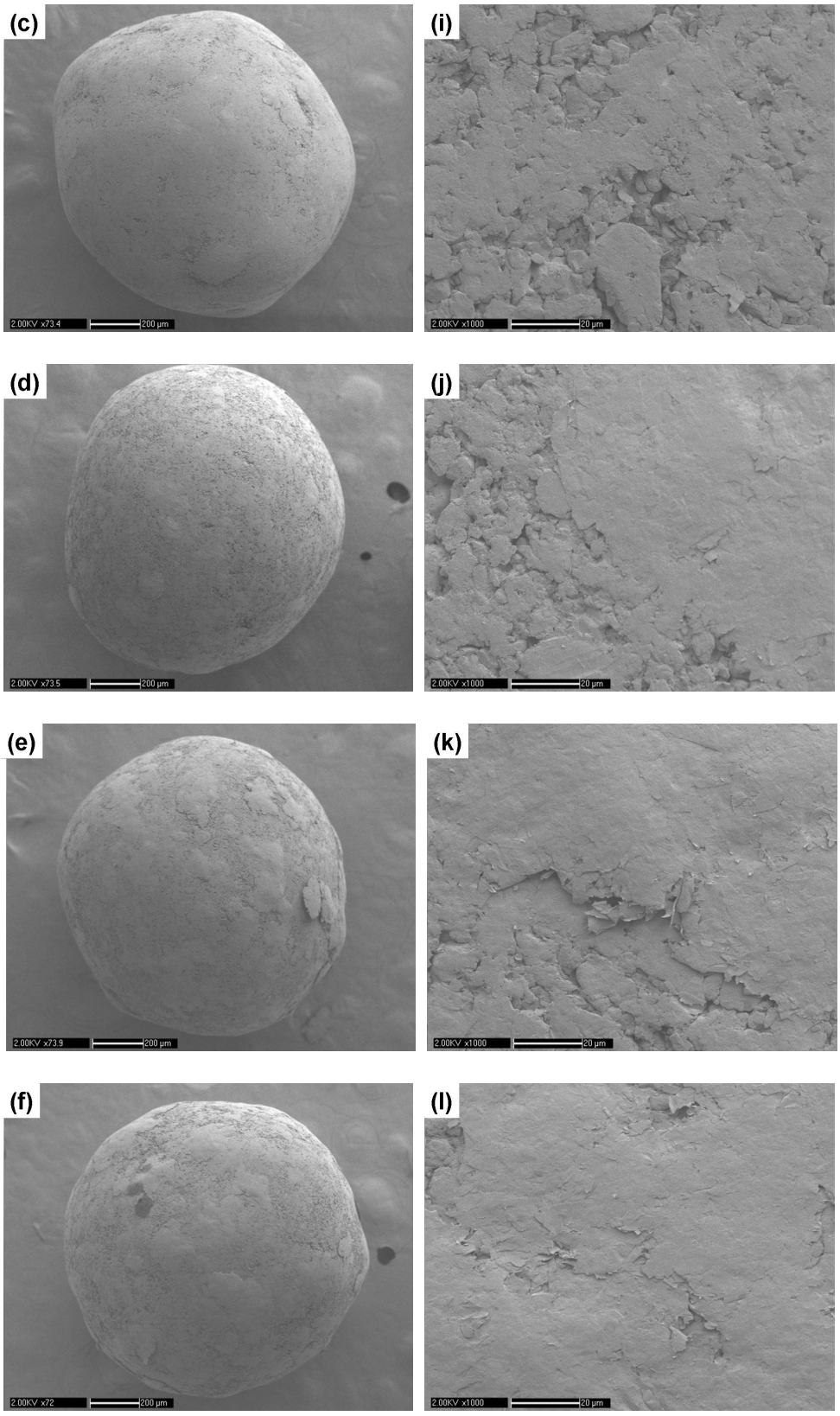

Fig. 4 SEM images of TATB-based PBXs samples with out-coating graphene: (a) PBX-R; (b) PBX-O-0.05; (c) PBX-O-0.15; (d) PBX-O-0.5; (e) PBX-O-1; (f) PBX-O-2; (g) PBX-R (high magnification); (h) PBX-O-0.05 (high magnification); (i) PBX-O-0.15 (high magnification); (j) PBX-O-0.5 (high magnification); (k) PBX-O-1 (high magnification); (l) PBX-O-2 (high magnification).

It is also observed from Fig. 2 that TATB-based PBXs show an increase in thermal conductivity with graphene content over the range of 0-2%. The thermal conductivity of PBX-R without graphene is measured to be 0.546 W/m·K. Compared to non-derivatised PBX, the thermal conductivity increases by 18.7% using 0.05% inner-coating graphene fillers. When the content of inner-coating graphene comes to 2 wt%, the thermal conductivity of TATB-based PBX increases to 1.122 W/m·K which is 1.06 times higher than PBX-R. Similar change trend of the thermal conductivity with graphene content is observed for the TATB-based PBXs with out-coating graphene. A scheme is proposed to present the microstructure of TATB-based PBXs without and with different concentration inner-coating and out-coating nanofillers (as shown in Fig. 5). Due to the high aspect ratio, graphene overlaps with each other in the composites. With lower concentration of graphene in nanocomposites, a very small quantity of contact points between graphene particles are established. The contact points between graphene particles remarkably increases with increasing graphene concentration to construct a network for thermal conductivity. It should be pointed out that the dependence of the thermal conductivity of TATB-based PBXs on graphene content is nonlinear. This is to be explained by the interaction among graphene in matrix together with the special properties of graphene such as high aspect ratio and ultra-high thermal conductivity[27].

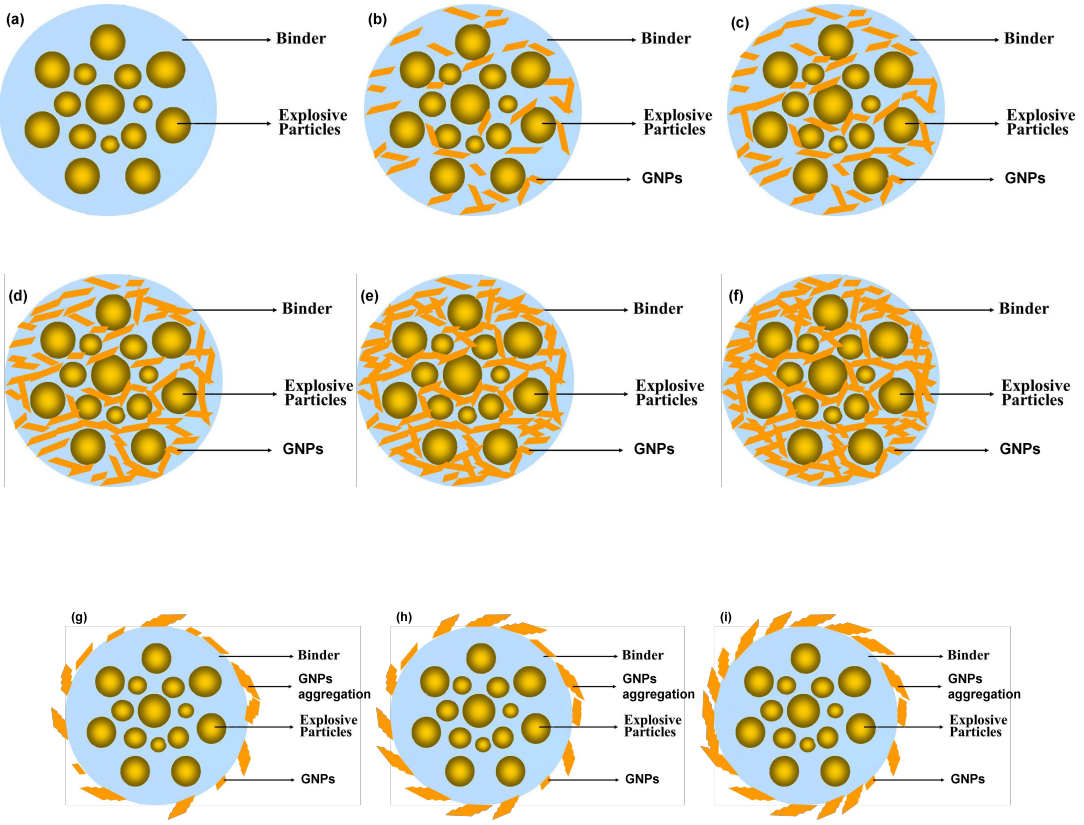

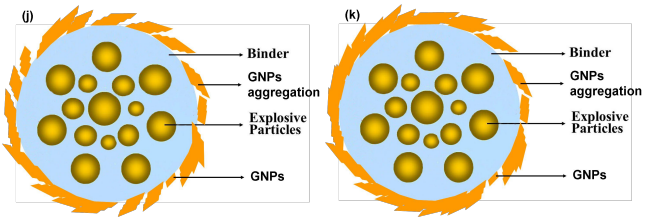

Fig. 5 The microstructural scheme in PBX with various weight ratios of graphene: (a) PBX-R; (b) PBX-I-0.05; (c) PBX-I-0.15; (d) PBX-I-0.5; (e) PBX-I-1; (f) PBX-I-2; (g) PBX-O-0.05; (h) PBX-O-0.15; (i) PBX-O-0.5; (j) PBX-O-1; (k) PBX-O-2.

3.2 Model analysis

PBXs are particles highly filled composite materials which are comprised of explosive crystallites as the filler material suspended in a polymeric binder as the matrix. In an attempt to deeply understand the thermal behavior of particles filled polymer composites, several theoretical models have been proposed to describe and prediction the thermal conductivity, such as Maxwell-Eucken, Bruggeman, Cheng-Vachon, and Nielsen-Lewis models[28-30]. Various empirical relationships are also established for the theoretical prediction of thermal conductivity. However, with high filler content, due to the fact that the contact of particles with each other leads to aggregation or the formation of thermal conductivity pathway, the models mentioned above could not well describe the experimental results. In addition, special attention should be paid to the influences of filler particles on the morphology of polymer materials. The limitations are solved with a new model given by Agari et al[31]. According to Agari model, thermal conductivity of composites in parallel and series conductions can be estimated using the following equations, respectively.

Parallel conduction for two-phase system (Fig. 6a):

$$\lambda_c = V_f\lambda_f + (1 - V_f)\lambda_p \qquad (1)$$

where λ_c is the thermal conductivity of the composite, V_f is the volume fraction of the filler in the composite, λ_p is the thermal conductivity of the polymer, and λ_f is thermal conductivity of the filler.

Parallel conduction for three-phase system with two different filler phases (Fig. 6c):

$$\lambda_c = V_{f1}\lambda_{f1} + V_{f2}\lambda_{f2} + (1 - V_{f1} - V_{f2})\lambda_p \qquad (2)$$

where V_{f1} and V_{f2} are the volume fractions of filler phases 1 and 2 in the composite, λ_{f1} and λ_{f2} are the thermal conductivity of two corresponding filler phases 1 and 2, respectively.

Series conduction for two-phase system (Fig. 6b):

$$\lambda_c = \frac{1}{V_f/\lambda_f + (1 - V_f)/\lambda_p} \qquad (3)$$

Series conduction for three-phase system with two different filler phases (Fig. 6d):

$$\lambda_c = \frac{1}{V_{f1}/\lambda_{f1} + V_{f2}/\lambda_{f2} + (1 - V_{f1} - V_{f2})/\lambda_p} \qquad (4)$$

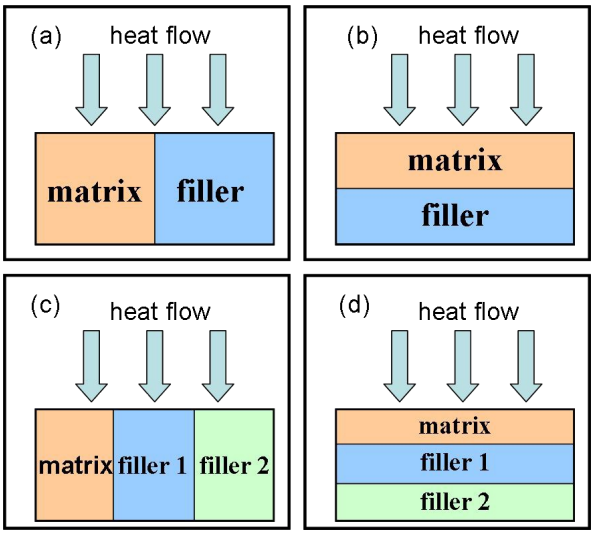

Fig. 6 Thermal conductivity model for polymer based composites: (a) parallel model of two-phase system, (b) series model of two-phase system, (c) parallel model of three-phase system, (d) series model of three-phase system.

For the system studied here, the thermal conductivity of the two-phase composite (PBX-R) and its continuous phase (fluoropolymer) and dispersed phase (TATB) are shown in Fig. 7a. The thermal conductivity of PBX-R is intervenient between TATB and fluoropolymer. For the graphene modified TATB-based PBXs, a new disperse phase (graphene) is introduced. The intrinsic thermal conductivity of graphene is reported to be 1500 ~ 3000 W/m·K[32], taken as 3000 W/m·K in this work. The Agari model is adopted to fit the experimental data of thermal conductivity and the results are shown in Fig. 7b-g. It can be seen from Fig. 7b that the modeling curves by the series model for two-phase system shows a satisfactory agreement with the experimental data at all temperatures examined with relatively errors of 0.04% to 2.60%. Wei et al.[33] have studied the thermal conductivity of HMX-based PBX and pointed out that the calculated values from the two-phase series model are in good agreement with the experimental results. As illuminated in Fig. 7c-g, the experimental thermal conductivity of graphene modified TATB-based PBXs are between the values calculated by three-phase series model and three-phase parallel model. It indicates that the thermal conduction mechanism of TATB-based PBXs with the addition of graphite changes from series model to partial parallel model, sequentially, the thermal conductivity of nanocomposites increases.

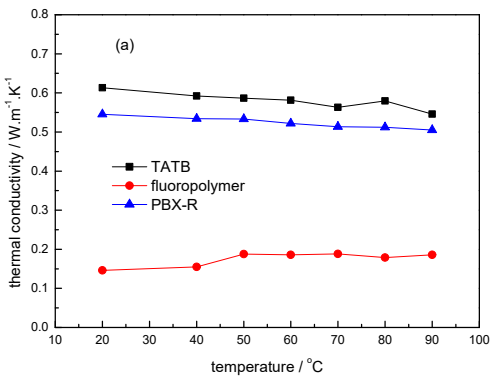

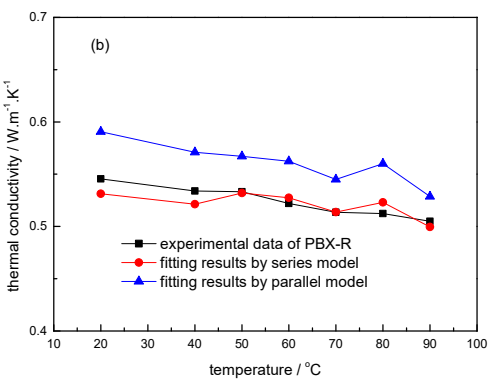

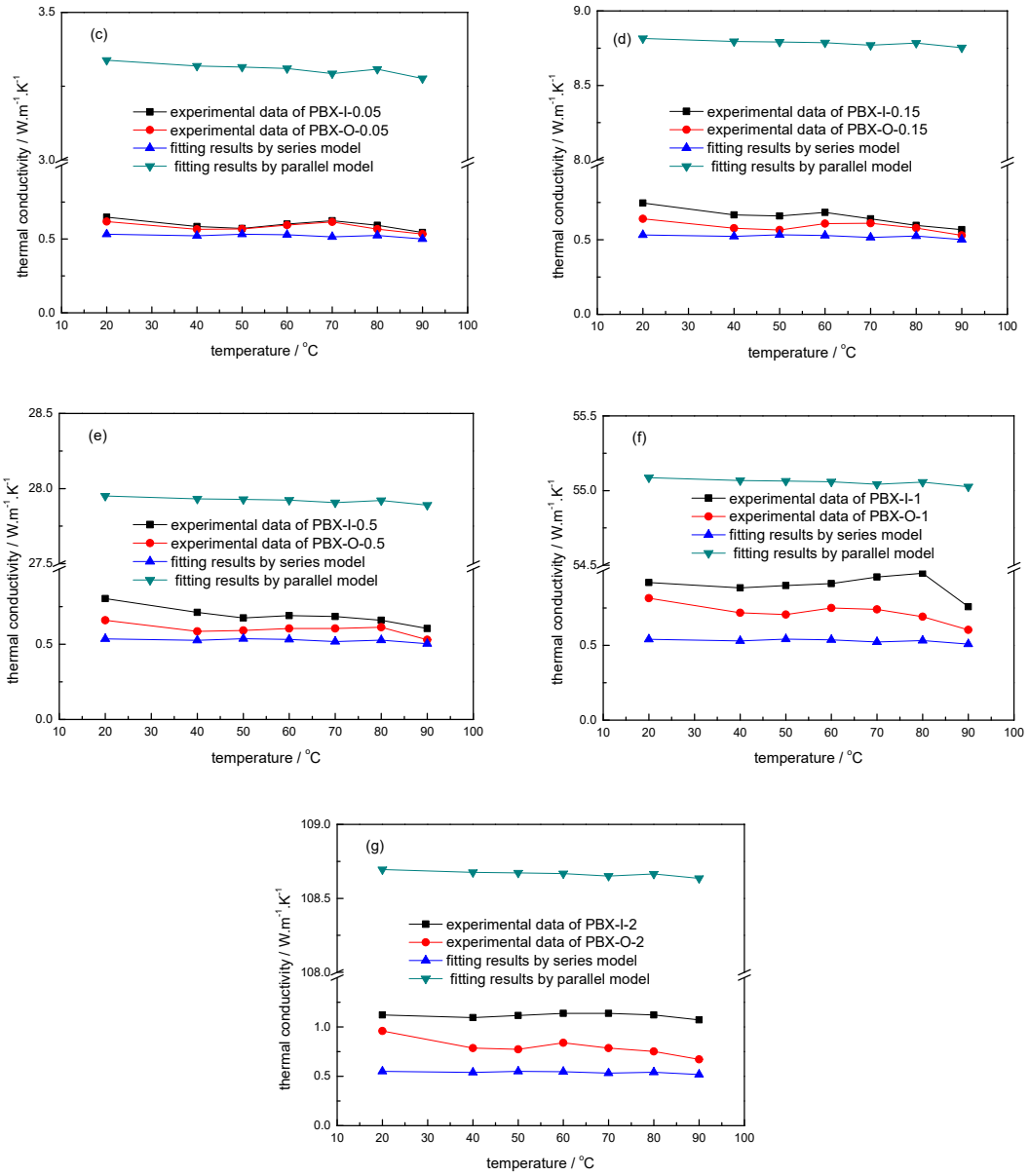

Fig. 7 Thermal conductivity curves and fitting curves of materials at different temperatures

3.3 Temperature dependence

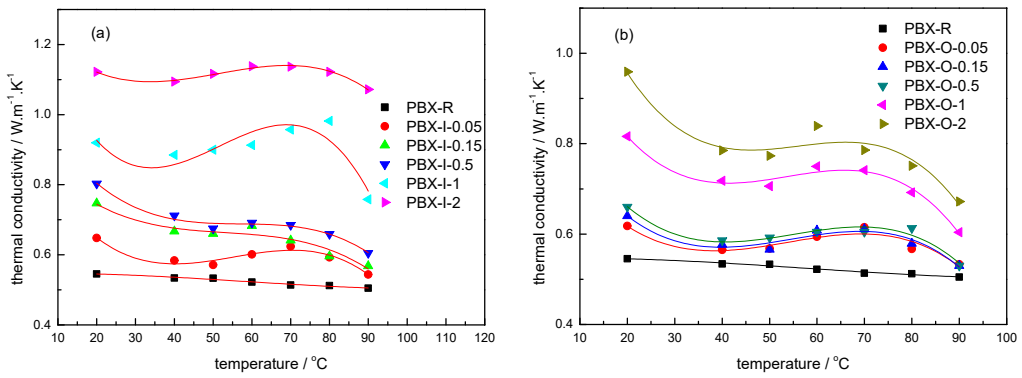

Fig. 8 Plots of thermal conductivity versus temperature of F2314/graphene composites

Fig. 8 gives the thermal conductivity versus temperature plots for all the samples. It can be seen that the temperature dependence of the thermal conductivity of TATB-based PBXs is non-linear. The thermal conductivity exhibits a sharp drop in the temperature domain from the 20 up to 40 °C. Then at higher temperatures from 50 to 70 °C, the thermal conductivity manifests almost no temperature dependence with a little fluctuation. Above 70 °C the thermal conductivity values decreased again. Generally, two competing effects of temperature on the thermal conductivity of PBX are functioning simultaneously on the nanocomposites: (i) the thermal conductivity of TATB (shown in Fig. 7a) and graphene[34] decreases with temperature. It has been found that the thermal conductivity of suspended high-quality graphene exceeds ~2,500 W/m·K at 350 K, and it is as high as ~1,400 W/m·K at 500K (experimental uncertainty ~40%)[35]. (ii) At the glass-transition peak of the polymer binder, thermal conductivity of polymer matrix reaches maximum, as given in Fig. 7a. This has been explained on the basis of predominant scattering processes[36]. Two competing or combined effects coexist in the TATB-based PBXs. The glass transition of fluoropolymer occurs at 50-70 °C[37,38]. Consequently, a little fluctuation is observed in the temperature range of 50-70 °C.

4. Conclusions

In this paper, 1,3,5-triamino-2,4,6-trinitrobenzene (TATB)-based polymer bonded explosives (PBXs) were modified with inner-coating and out-coating graphene. The influences of coating methods, graphene content, and temperature on the thermal conductivity of TATB-based PBXs were studied by a laser thermal conductivity apparatus. The following conclusions can be drawn:

(1) The preparation methods played an important role in the thermal behaviors of TATB-based PBXs. The ultrasound vibration stabilized a mixture of graphene and the polymer matrix solution against agglomeration, and facilitated better dispersion within the PBXs. Consequently, the PBXs with inner-coating graphene presented a higher thermal conductivity compared with the corresponding nanocomposites with out-coating graphene.

(2) The thermal conductivity of TATB-based PBXs was dependent on the graphene concentration and increased nonlinearly with its increase. The nonlinear dependence of the thermal conductivity of TATB-based PBXs on graphene content was attributed to the interaction among graphene in matrix together with the special properties of graphene.

(3) The thermal behaviors of TATB-based PBX and its graphene modified formulations were successfully evaluated using Agari model. The thermal conductivity of TATB-based PBX without graphene calculated from the Agari series model was in good agreement with the experimental data. The thermal conduction mechanism of TATB-based PBXs with inner-coating and outer-coating graphene was between Agari series model and parallel model.

(4) The dependence of the thermal conductivity of TATB-based PBXs on temperature was also investigated. The thermal conductivity exhibited a sharp drop in the temperature domain from the 20 up to 40 °C. Then at higher temperatures from 50 to 70 °C, the thermal conductivity manifested almost no temperature dependence with a little fluctuation. Above 70 °C the thermal conductivity values decreased again.

Acknowledgement

The authors are grateful to the Science and Technology Fund of CAEP (2015B0101011) and National Natural Science Foundation of China (11372290 and 11502245) for financial support.

References

1. D. Bedrov, G. D. Smith, and T. D. Sewell, *Chem. Phys. Lett.,* 2000, **324**, 64-68.
2. W. W. Erikson, M. A. Cooper, M. L. Hobbs, M. J. Kaneshige, M. S. Oliver, and S. Snedigar, *Int. J. Heat Mass Tran.,* 2014, **79**, 676-688.
3. R. K. Weese, A. K. Burnham, Heidi C. Turner, and T. D. Tran, *J. Therm. Anal. Calorim.,* 2007, **89**, 465-473.
4. P. W. Cooper and S. R. Kurowski, Introduction to the Technology of Explosives, New York: Wiley-VCH, p.21-23, 1996.
5. C. M. Ye, B. Q. Shentu, and Z. X. Weng, *J. Appl. Polym. Sci.,* 2006, **101**, 3806-3810.
6. S. U. S. Choi, Z. G. Zhang, W. Yu, F. E. Lockwood, and E. A. Grulke, *Appl. Phys. Lett.,* 2001, **79**, 2252-2254.
7. W. T. Hong and N. H. Tai, *Diam. Relat. Mater.,* 2008, **17**, 1577-1581.
8. M. J. Biercuk, M. C. Llaguno, M. Radosavljevic, J. K. Hyun, A. T. Johnson, and J. E. Fischer, *Appl. Phys. Lett.,* 2002, **80**, 2767-2770.
9. K. S. Novoselov, A. K.Geim, S. V. Morozov, D. Jiang, Y. Zhang, S. V. Dubonos, I. V. Grigorieva, and A. A. Firsov, *Science,* 2004, **306**, 666-669.
10. A. K. Geim and K. S. Novoselov, *Nat. Mater.,* 2007, **6**, 183-191.
11. M. Mirnezhad, M. Modarresi, R. Ansari, and M. R. Roknabadi, *J. Therm. Stresses,* 2012, **35**, 913-920.
12. L. Liu ,Y. Gao, Q. Liu, J. Kuang, D. Zhou, S. Ju, B. Han, and Z. Zhang, *Small,* 2013, **9**, 2466-2472.
13. X. Huang, F. Boey, and H. Zhang, *COSMOS,* 2010, **6**, 159-166.
14. R. Gu, W. Z. Xu, and P. A. Charpentier, *Polymer,* 2014, **55**, 5322-5331.
15. C. Heo, H. Moon, C. S. Yoon, and J. Chang, *J. Appl. Polym. Sci.,* 2012, **124**, 4663-4670.
16. F. Yavari, H. R. Fard, K. Pashayi, M. A. Rafiee, A. Zamiri, Z. Yu, R. Ozisik, T. Borca-Tasciuc, and N. Koratkar, *J. Phys. Chem. C,* 2011, **115**, 8753-8758.
17. S. Ganguli, A. K. Roy, and D. P. Anderson, *Carbon,* 2008, **46**, 806-817.
18. S. Yang, W. Lin, Y. Huang, H. Tien, J. Wang, C. M. Ma, S. Li, and Y. Wang, *Carbon,* 2011, **49**, 793-803.
19. C. Zhang, Y. Ma, and D. Jiang, *J. Mol. Model.,* 2012, **18**, 4831-4841.
20. R. H. Gee, S. Roszak, K. Balasubramanian, and L. E. Fried, *J. Chem. Phys.,* 2004, **120**, 7059-7066.
21. Z. J. Yang, J. S. Li, B. Huang, S. J. Liu, Z. Huang, and F. D. Nie, *Propell. Explos. Pyrot.,* 2014, **39**, 51-58.
22. J. T. Mang and R. P. Hjelm, *Propell. Explos. Pyrot.,* 2013, **38**, 831-840.
23. R. L. Gustavsen, R. J. Gehr, S. M. Bucholtz, R. R. Alcon, and B. D. Bartram, *J. Appl. Phys.,* 2012, **112**, 074909.
24. C. Souers, P. Lewis, M. Hoffman, and B. Cunningham, *Propell. Explos. Pyrot.,* 2011, **36**, 335-340.
25. W. Small IV, E. A. Glascoe, and G. E. Overturf, *Thermochim. Acta,* 2012, **545**, 90-95.
26. National Military Standard of China, Specific Heat, Thermal Conductivity, and Thermal Diffusion Using Laser Pulse Methods, GJB/772A-97, 1997 (in Chinese).
27. N. Shenogina, S. Shenogin, L. Xue, and P. Keblinski, *Appl. Phys. Lett.*, 2005, **87**, 133106.
28. O. H. Plast. Rubber Process, 1981, **1**, 9.
29. S. C. Cheng and R. I. Vachon. *Int. J. Heat Mass Tran.,* 1969, **12**, 249.
30. T. Lewis and L. Nielsen, *J. Appl. Polym. Sci.,* 1970, **14**, 449.

31. Y. Agari, A. Ueda, and S. Nagai, *J. Appl. Polym. Sci.,* 1994, **42**, 1665-1669.
32. K. Chu, C. Jia, and W. Li, *Appl. Phys. Lett.,* 2012, **101**, 121916.
33. X. Wei, X. Zhou, P. Wang, X. Tu, and X. Wang, *Chinese J. Explos. Propell.,* 2012, **35**, 33-37.
34. A. A. Balandin, *Nat. Mater.,* 2011, **10**, 569-581.
35. W. Cai, A. L. Moore, Y. Zhu, X. Li, S. Chen, L. Shi, R. S. Ruoff, *Nano Lett.,* 2010, **10**, 1645-1651.
36. R. Agarwal, N. S. Saxena, K. B. Sharma, S. Thomas, and M. S. Sreekala, *J. Appl. Polym. Sci.,* 2003, **89**, 1708-1714.
37. C. Lin, S. Liu, Z. Huang, G. He, F. Gong, Y. Liu, and J. Liu, *RSC Adv.,* 2015, **5**, 30592-30601.
38. C. Lin, J. Liu, S. Liu, Z. Huang, Y. Li, and J. Zhang, *Chinese J. Energ. Mater.,* 2015, **23**, 140-145.

A table of contents entry

The addition of graphene is a simple and novel route for improving thermal conductivity of polymer bonded explosives.